Available online at www.pelagiaresearchlibrary.com

Pelagia Research Library

Advances in Applied Science Research, 2012, 3 (6):4059-4065

ISSN: 0976-8610
CODEN (USA): AASRFC

High-speed signal processing in a programmable propagation simulator

E. Ehinlafa[a*], A. B. Shobo[b^], D. O. Kehinde [b+] and G. A. Ibitola[c**]

[a]*Department of Physics, University of Ilorin, Ilorin, Nigeria.*
[b]*Department of Basics Sciences, Babcock University, Ilishan-Remo, Nigeria.*
[c]*Department of Physics, Ondo State University of Science & Technology, Okitipupa, Nigeria.*

ABSTRACT

The real–time channel simulator described is an experimental apparatus designed not only for modelling a wideband channel, but also as a flexible machine for experimentation in propagation models and effects. In this paper, we describe the signal processing techniques used to model fading phenomena as well as the use of high-speed quadrature signal processing in the front-end of the simulator.

Key words: Propagation Simulator, Analog Signal Processing, Digital Signal Processing, Propagation Models, Wideband Channels.

INTRODUCTION

Cheap, reliable and repeatable tests of mobile communications gear are needed to check novel schemes of modulation and coding. For example, in order to test a new channel equalization algorithm, it is of critical importance that the algorithm be checked against a channel with varying types of impairments including fading and co-channel interference. Without a channel simulator, repeatable measurements are difficult, if not impossible. Furthermore, when a prototype is constructed, then we can get real- time measurements of the effects of channel “defects” on receiver performance. (See [1] for an example of such measurements).

This is particularly true in the “real world”, where propagation conditions are often intermittent and erratic.

Non-real-time (software) channel simulators have been designed and built for testing the effects of varying propagation on co-channel interference, handoff prediction, bit error rates and so forth. While non-real time simulators are beneficial for confirming the predicted performance of a given modulation and coding scheme, they do not permit the evaluation of real equipment with fundamental limitations of power, weight and finite word length; not to mention bugs.

The real-time channel simulator described in this paper is an experimental apparatus designed not only to model a wideband mobile channel, but also as a flexible machine for experimentation in propagation models and effects. To begin with, the underlying channel model will be described. Following this review, the signal processing algorithms, hardware and software will be given in detail.

PROPAGATION MODEL

Given a transmitted signal $\boldsymbol{T(t) = Re\{s(t)e^{j\omega_0 t}\}}$,

where **s(t)** is a complex valued information signal and $\boldsymbol{\omega_o}$ is the carrier frequency, the simulator's output must be

$\boldsymbol{R(t) = Re\{\rho(t)e^{j\omega_0 t}\}}$, where

$$\rho(t) = \sum_{k=1}^{\infty} \alpha_k s_k(t-\tau_k)e^{j\theta_k} + n(t) \qquad (1)$$

In this case, each path from a transmitter to a receiver is described by its fading function amplitude *(α_k)*, its carrier phase **(θ_k)** and its path delay *(τ_k)*. The added received noise $\{n(t)\}$ is a time-varying signal added to the attenuated transmitted signal. Each path can have a noise function as well as a general noise function that all signals are subject to, such as a noise source close to the receiver. The complex information signal for a given path can be written in its component parts as

$$s_k(t-\tau_k) = I_k(t-\tau_k) + jQ_k(t-\tau_k) \qquad (2)$$

For reasons to be discussed in the filter software section, the model requires the fading function to be complex valued. The model is illustrated in *Fig.1*.
It is possible to replace the fading function with the aggregate noise function of the model if the τ_k is set to an appropriate delay and α_k models the noise. The noise in each path can also be included in each α_k function. The fading model will be discussed in section 4.

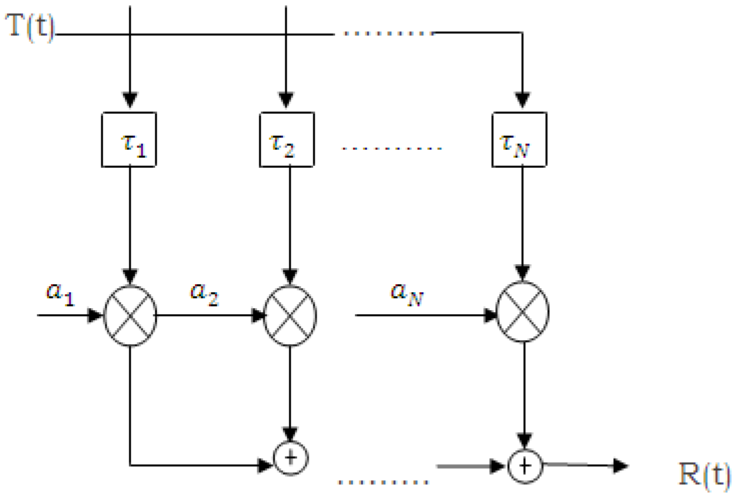

Figure 1: The Fading model

HARDWARE

Current cellular radio channels have a bandwidth of 6 MHz and are transmitted between 890 and 960 MHz. Therefore, the RF input signal must be down-converted before sampling. The 6 MHz bandwidth yields a 3 MHz baseband signal, and if the down modulation is performed to centre the down modulated signal around the baseband, a 10 MHz digital clock more than suffices for A/D conversion.

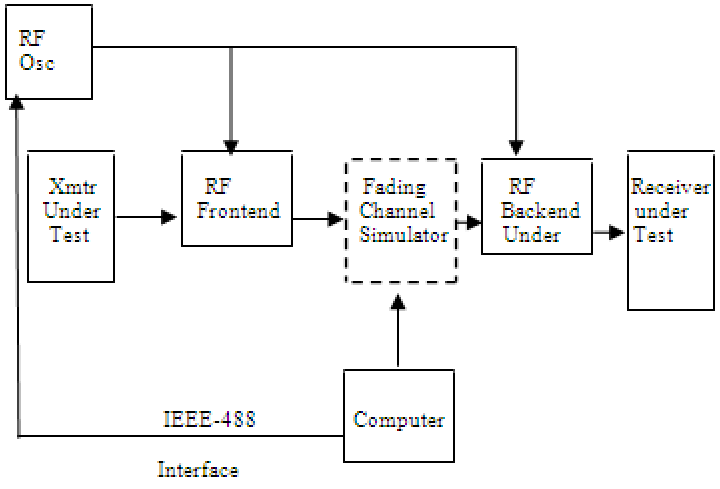

Figure 2: Simulator General Block Diagram

The RF oscillator is under the control of a workstation and is set to the proper frequency, depending on the transmitter carrier, to give the desired baseband into the analog-to-digital *(A/D)* converters that are part of the RF Frontend.

The RF front-end heterodynes the input down to a 70 MHz IF by mixing the oscillator output and the RF input from the transmitter under test. Following a 1.25 MHz SAW bandpass filter, the input signal is sampled by a fast *A/D* converter. The output of the converter is oversampled and filtered by a GrayChip GC1012 Digital Receiver under control of a small microprocessor. It outputs aligned I and Q channels [2]. The I and Q channels are run to the signal processor backplane via cables.

Schussler [3]-[4] uses an analog complex modulation scheme to derive the inphase and quadrature (1 and Q) components . Each of these is lowpass filtered and passed to separate *A/D* converters. Here, however, we use a completely digital complex mixer.

The fading channel simulator is made up of twelve cards, each of which simulates one of the possible paths from transmitter to receiver. If we allow the digitized signal input to the simulator to be described by $\boldsymbol{u(k) = I(k) + jQ(k)}$ and the fading function generated for each path to be given by $\boldsymbol{h_v(k)}$**,** then Figure 3 schematically shows the operation of one of the simulation cards.

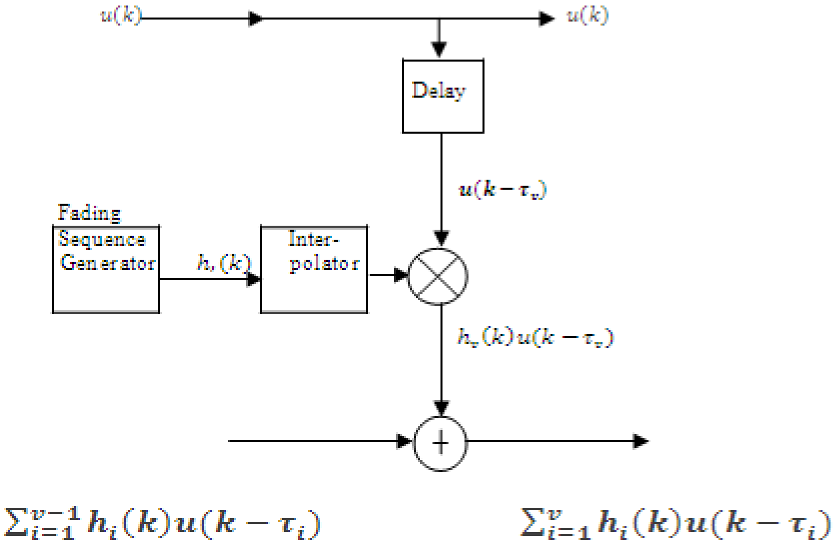
$u(k)$
$u(k)$
Delay
$u(k-\tau_v)$
Fading Sequence Generator
$h_v(k)$
Inter-polator
$h_v(k)u(k-\tau_v)$
$\sum_{i=1}^{v-1} h_i(k)u(k-\tau_i)$
$\sum_{i=1}^{v} h_i(k)u(k-\tau_i)$

Figure 3: Simplified Simulator Board

The Fading Sequence Generator provides a complex value every 1/256 of the system clock rate. The digital interpolator then provides an input to the multiplier on every clock cycle; however note that the output is just latched, thereby providing a zero-order hold [5]. There are two multipliers, one for I and one for Q. Similarly, there are two adders to add the output from the previous card with the current card in real-time.

At the end, the RF backend up-converts the simulator I and Q outputs back to RF, using the inverses of the above frequency conversion and sampling methods, so that the receiver under test can accept it as input.
The Fading Channel Simulator block diagram of Figure 2 can then be given as Figure 4 where each block, *v*, performs the function of Figure 3.

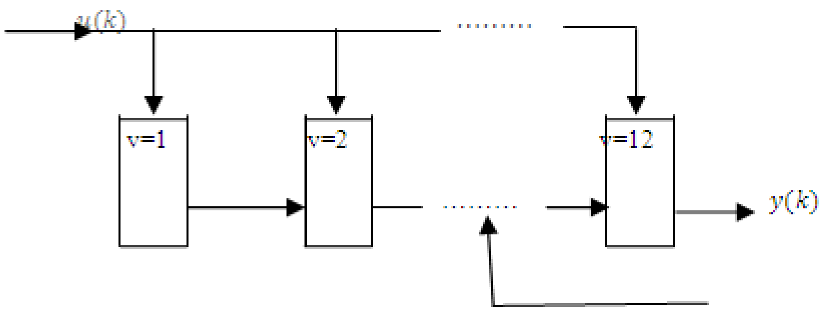

$$\sum_{i=1}^{v} h_i(k)u(k-\tau_i)$$

Figure 4: The Fading Channel Simulator

SOFTWARE

4.1 Fading coefficient generation

The Fading Sequence Generator of Fig. 3 is modeled as shown in Figure 5.

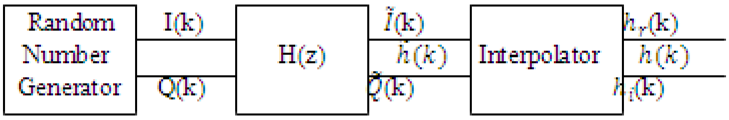

Figure 5: The Fading Sequence Generator

The statistical averages of the fading functions are Rayleigh distributed. Such a process can be simulated by choosing two numbers, one for I and one for Q, with mutually independent Gaussian statistics that have zero mean and equal unit variance. The Random Number Generator of Figure 5 takes uniformly distributed and independent white noise random numbers and converts them into Gaussian distributed random numbers by shuffling and adjusting the mean. A pair of these Gaussian numbers is taken to be the real and complex (I and Q) parts of the fading sequence. However, these numbers alone do not lead to power spectra for the process that agree with measured data. Therefore, the transfer function, *H (z)*, must transform the power spectra into one that corresponds to the environment, including the type of antenna in use and the speed of the vehicle. Both Clarke [6] and Bajwa and Parsons [7] have verified the received power spectrum at an antenna can be represented by one of the three power spectra in Figure 6.

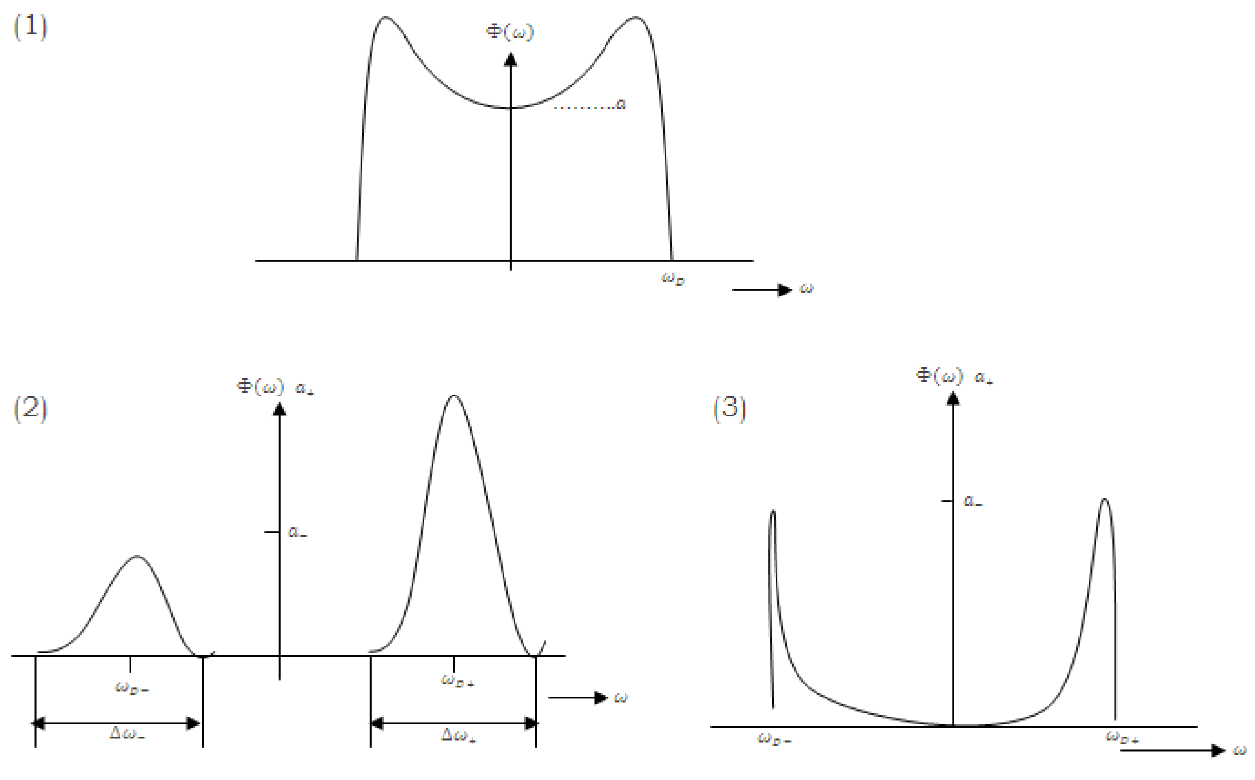

Figure 6: The Fading Model Power Spectra

Case number one is the typical spectrum that a vertical monopole antenna receives from a line of sight transmission or from a large amount of local scattering. Its power density spectrum, $\Phi(\omega)$, is approximated by

$$\Phi(\omega) = \begin{cases} \frac{a_v}{\sqrt{1-(\omega/\omega_D)^2}} & |\omega|<\omega_D \\ 0 & |\omega|>\omega_D \end{cases} \qquad (3)$$

where ω_D is the Doppler frequency (*f* from equation (1) times *2π)* and α is its amplitude.

The second case of Fig. 6 occurs when signals come from directly ahead of or behind a moving train of pulses. The power spectra is approximated by a Gaussian shape

$$\boldsymbol{\Phi(\omega) = e^{-x^2}/2} \qquad (4)$$

that is shifted by the Doppler frequency ω_D. Note that the spectra can be non-symmetrical about ω= 0. Therefore, to simulate this power spectra, one must specify the two Doppler frequencies, ω_{D-} and ω_{D+}, the bandwidth of each spectra, $\Delta_{\omega-}$ and $\Delta_{\omega+}$, and the amplitude a+ and a_, of each spectrum.

Finally, the third spectrum in Fig. 6 occurs when echoes also incur scattering. It also represents the spectra seen by a vertical loop antenna in the plane of vehicle motion. It is characterized by:

$$\boldsymbol{\Phi(\omega) = a}\frac{(\omega/\omega_D)^2}{\sqrt{1-(\omega/\omega_D)^2}}$$

Note that it can also be asymmetrical about ω=0; so two amplitudes, a+ and a_, and two Doppler frequencies, ω_{D-} and ω_{D+}, must be specified.

With regard to equation (1), and the fact that mobile channels lie in the 890-960 MHz carrier range, it is possible to implement the power spectra shaping as either lowpass or bandpass digital filters. A higher carrier frequency would have a higher Doppler shift for a vehicle traveling at some velocity. Then, in modeling an environment at maximum shift conditions, that is, using 960 MHz carrier with a mobile velocity of 80 Miles/hour (128.7 Km/hour) and all waves coming from in front of or behind the mobile train $(cos(\alpha)$ = 1), the Doppler shift would be only 411.8 Hz (2.589 K-rad). This justifies the feasibility of the lowpass/bandpass model.

Then, to simulate the first function in Fig. 6, it is possible to filter each of the noise sources with identical low pass filters, resulting in equal power spectra out for both the imaginary and real components. The Gaussian distributed noise generator supplies numbers that have identical power spectra to the input of each channel. It is not trivial, however, to generate the asymmetric spectra of the second and third functions of Figure 6. Lowpass filters (and bandpass filters that are transformed to lowpass filters) are symmetric about ω = 0. Schussler describes the necessary operation as a Hilbert transformer implemented as two all-pass filters, each of which shapes either the upper half or the lower half of the filter spectrum. What is actually done is a complex modulation of the filtered real and imaginary parts to remove unwanted sidebands and join the two desired spectra together. The *H (z)* block of Figure 5 can then be realized by figure 7:

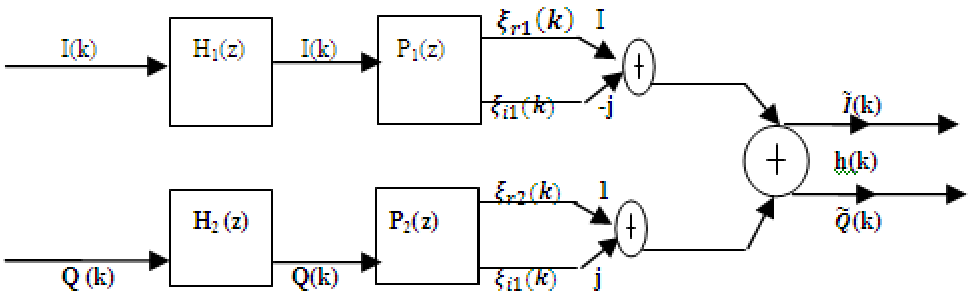

Figure 7: The Filter Model, H(z)

In Fig. 7, the filter functions $H_1(z)$ and $H_2(z)$ are symmetric lowpass or bandpass filters. At a minimum, they are fourth order. Their outputs can be labeled $\tilde{I}(k)$ and $\tilde{Q}(k)$ for the first filter model of Fig. 6. However, for the other two filter models, the rest of the network of Fig. 7 is required. P_1 and P_2 are all-pass phase splitting networks (see Gold and Rader [8] for the details including state diagram and coefficients derivation). The gain for each branch in the network is unity but the outputs, ξ_{r_i}(k) and ξ_{i_i}(k) are exactly 90° out of phase. By adding the outputs of P_1 (ξ_{r_1} and ξ_{i_1}) in the manner shown (ξ_{r_1}- jξ_{i_1}), pthe spectrum for ω > 0 is obtained and the spectrum for ω < 0 is zero. Also, by adding the outputs of P_2, the spectrum for $\omega < 0$ is obtained while the spectrum for $\omega > 0$ is zero. Then, the desired output spectrum *h(k)* {for Fig. 6, parts (2) and (3)} is obtained by adding the upper and lower frequency parts together. Note then that $H_1(z)$ shapes the frequency response for $\omega > 0$ and $H_2(z)$ shapes the frequency response for $\omega < 0$. Also note that the frequency response of the functions in Fig. 6, parts (2) and (3) have zero magnitude at $\omega = 0$.

4.2. Software library

The fading coefficients are generated on a Digital Signal Processor DSP32C - ATT. With a 40 MHz clock, it has a 100 - ns cycle time and when effectively pipelined, can perform 10 MegaMAcs (where MAc = Multiply Accumulate) per second.

The output sample clock for the DSP-32C-ATT is generated by either an external oscillator or dividing down 10 MHz by 256 (to obtain f ≈39 KHz). The output of the DSP is latched before going to the complex multiplier. Since the sampling rate of the DSP is so slow, the fading output can use the serial port of the DSP.

The DSP program is cross-compiled on the workstation and saved in a library. Depending on the fading function and noise environment desired, a different fading function can be loaded into the DSP's fast static program memory via the parallel interface shown in Fig. 2.

Given the 39 KHz sampling rate of the fading channel and the 10 MHz instruction clock (there are 4 minor cycles per instruction), then the DSP can execute approximately 256 instructions in the sample loop. These cycles are divided into fading computation and noise computation. Obviously, the programs must fit within the tight time bounds of the sample clock. Slower sample rates clearly permit larger programs.

CONCLUSION

The novel features of this simulator include the fully digital means of dividing the inphase and quadrature inputs and generating quadrature outputs. A large dynamic memory in the computer interface enables the capture of input and output data for further analysis, while the fully digital quadrature processing effectively eliminates phase errors and overwrought RF processing. The high-speed programmable propagation simulator can process analogue signals at several MHz and can process digital signals at over 40 kB/s.

REFERENCES

[1]. M. R. L. Hodges, S. A. Jensen and P. R. Tattersall, *Br. Telecom Technol. J.*, Laboratory testing of digital cellular radio systems, **Jan. 2010**, 8, 1 pp. 57-66.

[2]. R. L. Mitchell, *IEEE Transactions on Aero. and Elect. Systems*, Creating complex signal samples from a band-limited real signal, **May 2002**, *AES-25*, 3 pp. 425-427.

[3]. H. W. Schiissler, J. Thielecke, K. Preuss, H. Brehm and M. Werner, *An Intermediate Report about the State of the Development*, A Digital Frequency-Selective Fading Simulator, Lehrstuhl fur Nachrichtentechnik, Universitat Erlangen-Numberg, **Dec. 2003**.

[4]. H.W. Schussler, J. Thielecke, K. Preuss, W. Edler and M. Gerken, *J. Frequenz* A Digital Frequency-Selective Fading Simulator, **Jan. 2001**, 43, 2, pp. 47-55.

[5]. R. Fitzgerald and W. Anderson, *IEEE Trans. ASSP*, Spectral Distortion in Sample Rate Conversion by Zero Order Polynomial Interpolation, **June 2007**, ASSP-40, 6 , pp. 1576-1578.

[6]. R. H. Clarke, *A Statistical Theory of Mobile-Radio Reception*, B.S.T.J., **July -August 1995**, pp. 957-1000.

[7]. J. D. Parsons and A. S. Bajwa, *IEE Proceedings*, Small-Area Characterization of UHF Urban and Suburban Mobile Radio Propagation, **April 2007**, Part F-129, 2, pp. 102-109.

[8]. B. Gold and C. M. Rader, *Digital Processing of Signals*, McGraw-Hill, **1999**.

[9]. Parsons, J.D.: “*Digital Signal Processing*”, http://www.dspelectronics.com **2009**.